

Wing kinematics of avian flight across speeds

Bret W. Tobalske, Tyson L. Hedrick and Andrew A. Biewener

Tobalske, B. W., Hedrick, T. L. and Biewener, A. A. 2003. Wing kinematics of avian flight across speeds. – J. Avian Biol. 34: 177–184.

To test whether wing shape affects the kinematics of wing motion during bird flight, we recorded high-speed video (250 Hz) of four species flying in a variable-speed wind tunnel. The birds flew at intervals of 2 m s^{-1} , ranging from 1 m s^{-1} up to their respective maximum flight speed, which varied from 14 to 17 m s^{-1} depending on the species. Kinematic data obtained from two synchronized, high-speed video cameras were analyzed using 3D reconstruction. Three species with relatively pointed, high-aspect ratio wings changed wingbeat styles according to flight speed (budgerigar, *Melopsittacus undulatus*; cockatiel, *Nymphicus hollandicus*; ringed turtle dove, *Streptopelia risoria*). These species used a wing-tip reversal upstroke, characterized by supination of the distal wing at mid-upstroke, at equivalent airspeeds ≤ 7 to 9 m s^{-1} . In faster flight, they used a swept-wing upstroke, without distal wing supination. At mid-upstroke at any speed, wingspan in these species was greater than wrist span. In contrast, at all steady flight speeds, the black-billed magpie *Pica hudsonia* with relatively broad, low-aspect ratio wings, used a flexed-wing, feathered upstroke in which wrist spans were equal to or greater than wingspans. Our results demonstrate that wing kinematics vary gradually as a function of flight speed, and that the patterns of variation are strongly influenced by external wing shape.

B. W. Tobalske (correspondence) Department of Biology, University of Portland, 5000 N. Willamette Boulevard, Portland, OR 97203, USA. T.L. Hedrick and A.A. Biewener, Concord Field Station, Museum of Comparative Zoology, Harvard University, Old Causeway Road, Bedford, MA 01730, USA. E-mail: tobalske@up.edu

A wealth of data exists for the patterns of wing movement observed in bird flight for species flying at one speed or over a limited range of speeds (e.g. Brown 1963, Scholey 1983, Tobalske and Dial 2000). Although birds may vary aspects of their downstroke according to flight speed (Park et al. 2001), in general it appears that upstroke kinematics are more variable than downstroke kinematics. Birds with rounded, low-aspect ratio wings are usually observed using a highly flexed wing posture with a “feathered” upstroke in which the primary feathers are separated only slightly and resemble a venetian blind as the wing is elevated. Exceptions to this pattern include the Galliformes (Brown 1963, Tobalske and Dial 2000). Birds with pointed, high-aspect ratio wings use a “tip-reversal” upstroke at slow speeds, in which the wrists are adducted and the distal wings are supinated. These species do not employ tip reversal in fast flight; rather they abduct their wrists and adopt a “swept-wing” distally during upstroke. The transition between tip-reversal and swept-wing patterns across

flight speeds has previously been studied for only one species, the pigeon (*Columba livia*; Brown 1953, Tobalske and Dial 1996). It appears that the transition in this species occurs near 10 m s^{-1} (Tobalske and Dial 1996).

Wing movements are of interest because aerodynamic mechanisms, neuromuscular control, respiratory patterns, and demands upon skeletal design are hypothesized to be associated with different wingbeat styles (Rayner 1991, 1995, Tobalske 2000). These hypotheses remain largely untested, in part because of a lack of useful comparative data on wing kinematics.

To begin to address this need for comparative data, and to test the hypothesis that wing shape affects the wingbeat style of flying birds, we obtained measurements of wing motion from four species trained to fly in a new, variable-speed wind tunnel: budgerigar *Melopsittacus undulatus*, cockatiel *Nymphicus hollandicus*, ringed turtle dove *Streptopelia risoria* (hereafter “dove”) and black-billed magpie *Pica hudsonia* (hereafter “magpie”).

Materials and methods

Animals and training

Budgerigars (31.7 g, $n = 2$), cockatiels (78.5 g, $n = 2$), and doves (139.8 g, $n = 2$) were obtained from a licensed animal dealer (Table 1). Magpies (187.7 g, $n = 2$) were wild-caught in Missoula, Montana, USA and used on temporary loan from K. Dial and M. Bundle. When not being trained in the wind tunnel the birds were housed in small indoor/outdoor aviaries, measuring $2.5 \times 2.2 \times 5$ m. All training and experiments took place at the Concord Field Station (CFS), Harvard University, Bedford, MA, USA (41 m altitude above sea level, average air density 1.2 kg m^{-3}). None of the birds were in moult during the experiments, and all remiges and retrices were undamaged.

Morphometric data were collected from the birds immediately after conducting the experiments (Table 1). Body mass (g) was measured using a digital balance. We used conventional methods to obtain wing measurements (Pennycuik 1989, Tobalske 1996). Single wing length (cm), wing span (cm) and wing area (cm^2 ; including projected area of both wings and the body between the wings) were measured with the wings fully extended and with the feathers spread as in mid-down-stroke of flapping flight. We verified the mid-down-stroke posture from video images obtained during flight. In this posture, the emargination on the distal third of each of the primaries was completely separated from adjacent feathers. Wing length was measured along a straight line from the ventral surface of the shoulder to the distal tip of the 9th primary, and wing span was measured along a straight line, between the distal tips of the 9th primaries, with the bird ventral side up. Wing area was obtained from wing and body tracings. Each wing was stretched over the side of a table, dorsal side up, with the edge of the table abutting the shoulder of the bird (Pennycuik 1989). The outline of the stretched wing, including all feathers distal to the proximal end of the humerus, was traced onto paper and the tracing was imported to a computer via a digital camera (Olympus D400-zoom). The digital image of the wing outline was then traced using NIH

Image software, and wing area was converted from pixels within the wing outline to cm^2 using a known scale. Both wings from each bird were measured in this way. We used similar methods to measure the projected surface area of the body between the wings, but the outline of the body was traced with the bird laying ventral side up. The area of the body included in our measure of wing area was defined cranially by the leading edge of the wing and caudally by the trailing edge of the longest secondaries.

Average wing chord (cm) was calculated as wing area divided by wingspan. Aspect ratio (dimensionless) was calculated as wingspan divided by wing chord. Disc loading (N m^{-2}) was computed as body weight divided by disc area (S_d). We assumed $S_d = \pi b^2$, with b = half span of the wings. Wing loading (N m^{-2}) was computed using body weight (N) divided by combined wing area, including the projected surface area of the body between the wings.

Bird training initially involved brief, repeated flights with the birds taking off from a hand-held perch. Individual training sessions typically lasted 15 to 20 min for each bird and were often repeated a second time each day (separated by an intervening period of rest lasting no less than two hours for each bird). As training progressed, the duration of the flights was increased until the birds would voluntarily fly in the working section with the floor and side port doors closed. This was done at a wind speed that the birds seemed most comfortable (8 to 10 m s^{-1}). Once the birds would voluntarily fly for minutes at a time at this speed, they were trained to extend their speed range to both slower and faster speeds. After training, all four species would fly at 1 m s^{-1} . Maximum speeds were 13 m s^{-1} in magpies, 15 m s^{-1} in budgerigars and cockatiels, and 17 m s^{-1} in doves.

Wind tunnel

The Harvard-CFS tunnel, completed in 1999, is an open circuit (flow-through) system with a 6:1 contraction ratio and a $1.2 \times 1.2 \times 1.4$ m working section

Table 1. Morphological data for bird species used for kinematic study: budgerigar, cockatiel, ringed turtle-dove and black-billed magpie. Included are means \pm S.D.; $n = 2$ birds for each species.

| Variable | Species | | | |
|------------------------------------|-----------------|------------------|--------------------|---------------------|
| | Budgerigar | Cockatiel | Ringed Turtle-Dove | Black-billed magpie |
| Body Mass (g) | 31.7 \pm 2.1 | 78.5 \pm 2.8 | 139.8 \pm 15.4 | 187.7 \pm 2.1 |
| Single wing length (cm) | 13.0 \pm 0 | 22.2 \pm 0.4 | 21.3 \pm 1.0 | 25.6 \pm 1.5 |
| Wing span (cm) | 29.0 \pm 0 | 48.3 \pm 1.3 | 46.8 \pm 0.8 | 59.9 \pm 4.6 |
| Average wing chord (cm) | 4.0 \pm 0.1 | 6.9 \pm 0.4 | 8.2 \pm 0.1 | 11.9 \pm 0.3 |
| Aspect ratio | 7.3 \pm 0.1 | 7.0 \pm 0.2 | 5.7 \pm 0.1 | 5.0 \pm 0.3 |
| Wing area (cm^2) | 116.0 \pm 1.5 | 332.7 \pm 28.8 | 385.4 \pm 10.5 | 711.8 \pm 73.8 |
| Wing loading (N m^{-2}) | 26.8 \pm 1.4 | 23.2 \pm 1.2 | 35.6 \pm 3.0 | 26.0 \pm 2.4 |
| Disc loading (N m^{-2}) | 4.7 \pm 0.3 | 4.2 \pm 0.1 | 8.0 \pm 0.6 | 6.6 \pm 0.9 |

walled with clear Lexantm. Driven by a DC motor and direct-drive fan, the tunnel is capable of moving air through the working section at continuous increments of speed up to 28 m s⁻¹. Full details of tunnel design and performance are provided in Hedrick et al. (2002). In brief, at an airspeed of 20 m s⁻¹, variation in flow velocity is less than 2.5% of the mean wind speed and averages 0.7% (mean ± S.D. = 20.0 ± 0.14 m s⁻¹). Effects of the boundary layer on wind velocity are not appreciable until within 1 cm of the wall. Airspeeds remain within 1.5% of mean wind speed over the span of the section to within a distance of 2 cm of the right and left walls. Tunnel turbulence, measured using a turbulence sphere (Hoerner 1935, Barlow et al. 1999) is less than 1.28%, averaging 1.10 ± 0.08%.

For our experimental results, we follow Pennycuik et al. (1997) in reporting *equivalent* wind speed (V_e) rather than true wind speed:

$$V_e = \sqrt{2q/\rho_o}$$

where q is dynamic pressure and ρ_o is air density at sea level (1.225 kg m⁻³).

High-speed video recording

Digital video recordings were obtained of the birds at 250 frames s⁻¹ using two synchronized (pixel capture 480 × 420) Redlake PCI-500 cameras. Shutter speed was 1/2500 s. One camera was positioned lateral to the working section and the other camera above and behind the working section mounted on a support attached to the ceiling of the room. Both cameras were equipped with an 8 × 48 zoom lens that provided a full-field view that was approximately two times greater than the bird's wing span.

We studied wing and body motion by digitizing anatomical landmarks (dorsal midline, shoulder, wrist, elbow, wingtip at distal end of 9th primary, base and tip of outer retrices of tail) in successive fields of video. Methods were similar to those used in Hedrick et al. (2002). Wing and tail locations were marked using 5-mm diameter circles of white tape marked with a black center dot. Four-point crosses of 3-mm wide white tape with black dots at the tips was used to identify the dorsal midline. Individual sequences of flight were selected from the video data and digitized using custom software written in Matlab v5.3 (The MathWorks, Inc.).

In our measurements of flight kinematics, we included successive wingbeats that periodically featured changes in a bird's altitude and velocity; however, maneuvering phases, including yaw or roll, were excluded. To obtain kinematic measures, we merged two-dimensional (2D) coordinates from each camera

plane into a single three-dimensional (3D) space using the Direct Linear Transform (DLT) coefficients derived from a nineteen-point calibration frame (Hatze 1988). In addition to merging the separate 2D camera views into a single 3D coordinate space, the DLT method also compensates for parallax and other lens distortions. Individual points having a DLT root mean square (RMS) error two standard deviations greater than the median error for that point were removed prior to analysis. For all birds tested, median RMS error was 2.3 mm for the dorsal midline and 7.7 mm for the wingtip. Occasionally a point was not in the view of both cameras, resulting in a gap in the reconstructed point sequence. Point interpolation and filtering were accomplished with a quintic spline fit to known RMS error using the Generalized Cross Validatory/Spline (GCVSPL) program (Woltring 1986, Walker 1998). This method uses RMS error from the DLT reconstruction to filter the positional data, and then fills any gaps with a quintic spline interpolation. The results from this technique were similar to those obtained by smoothing the positional data using a 37 Hz digital Butterworth low-pass filter. As a test of the accuracy of the 3D reconstruction, filtering, and derivation methods, a five-mm ball bearing was bounced in the video recording field. Derivation of gravitational acceleration from the motion of the bearing resulted in a value of 9.79 m s⁻², reasonably close to the universal value of 9.81 m s⁻².

Using 3D reconstruction, we obtained simple metrics that are directly comparable with prior 2D efforts to characterize flight kinematics (Tobalske and Dial 1996, 2000) or which have been suggested to correlate with aerodynamics (Tobalske 2000). We measured wingspan and wrist-span at mid-upstroke and mid-downstroke, with the phase of the wingbeat cycle defined according to elevation or depression of the tip of the 9th primary relative to the shoulder. Distal-wing angle was the perceived angle at mid-upstroke between the wrist-tip segment and the long axis of the body from a lateral projection. We also measured the body angle relative to horizontal and velocity and acceleration of the body.

Although patterns generally suggest continuous variation in mid-upstroke postures, for convenience in our discussion of these patterns we attempt to categorize upstrokes as being feathered, tip-reversal, or swept-wing. We classified feathered and swept-wing upstrokes according to distal-wing angles being less than 30°. However, compared with wrist span in mid-downstroke, wrist-span at mid-upstroke is < 40% in feathered upstrokes and > 70% in swept-wing upstrokes. Tip-reversal upstrokes are defined as those with wing span at mid upstroke ≥ 50% of mid-downstroke span and distal-wing angle ≥ 30°. In discussing wing kinematics, we report means ± S.D.

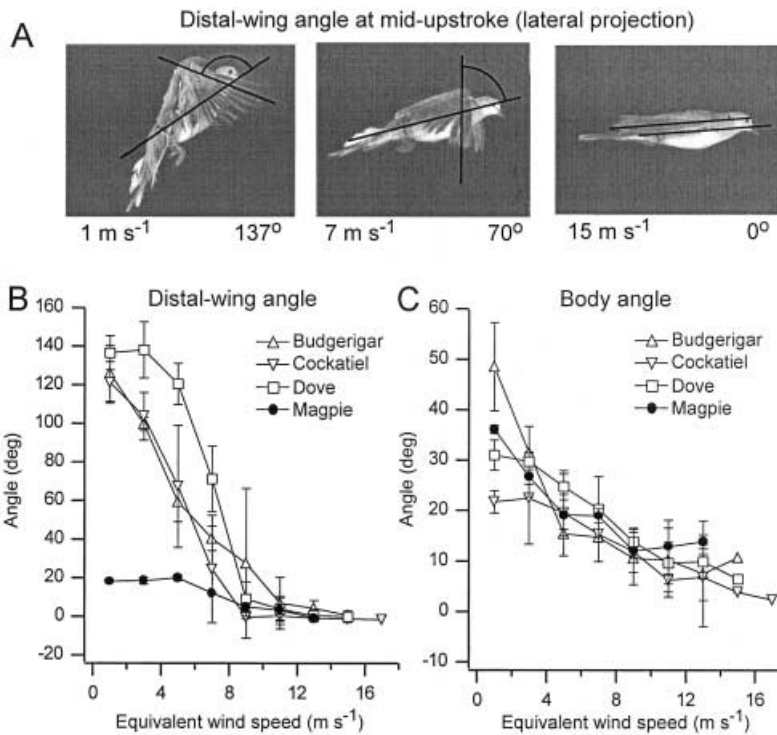


Fig. 1. Variation in distal-wing and body angles, viewed at mid-upstroke from a lateral projection, as a function of equivalent airspeed up to 17 m s⁻¹ in budgerigars, cockatiels, ringed turtle doves, and black-billed magpies. We interpret a distal-wing angle greater than 20° to represent a wing-tip reversal upstroke. A) Single video fields, from sequences obtained at 250 Hz, showing mid-upstroke posture in the ringed turtle-dove at three different equivalent airspeeds. B) Variation in distal-wing angle relative to midline of the body in the four species. C) Body angle relative to horizontal. Error bars represent \pm S.D.

Results

With increasing flight speed, there was a general pattern of decreasing distal-wing angle relative to the midline of the body, and decreasing body angle relative to horizontal, among all of the species in this study (Fig. 1). However, clear differences were apparent for distal-wing angles of magpies compared with those of the other species when engaged in slow flight. At all flight speeds, magpies used feathered upstrokes without significant supination of their distal wings ($< 20^\circ$). In contrast, budgerigars, cockatiels, and doves exhibited wing-tip reversal upstrokes at speeds from 1 to 7 m s⁻¹ (Fig. 1). Over this range of speed, distal-wing angle was slightly higher in the dove compared with the budgerigars and cockatiels. Distal-wing angle was less than 10° for the doves and cockatiels at speeds ≥ 7 m s⁻¹ and for the budgerigar at speeds ≥ 9 m s⁻¹. At 7 and 9 m s⁻¹, these three species exhibited modulation in upstroke posture, with tip-reversal wingbeats alternating with swept-wing wingbeats (Fig. 2).

At intermediate speeds (7 to 9 m s⁻¹), all four of the species tended to exhibit regular fluctuations in body altitude and velocity, associated with observable changes in wing kinematics. Among the species that used wing-tip reversal during upstroke, distal-wing angle also varied with wingbeat frequency and vertical acceleration of the body. Fig. 2 shows an example of a dove flying at an average V_e of 7 m s⁻¹. In this flight sequence, lasting two seconds, the largest intra-wing-

beat vertical accelerations of the body are associated with wingbeats in which the distal-wing angle exceeded 100° at mid-upstroke. Wingbeat frequency during these accelerative bursts averaged 9.9 Hz compared with an average of 6.4 Hz during steady or decelerative wingbeats in the sequence. Magpies, on the other hand,

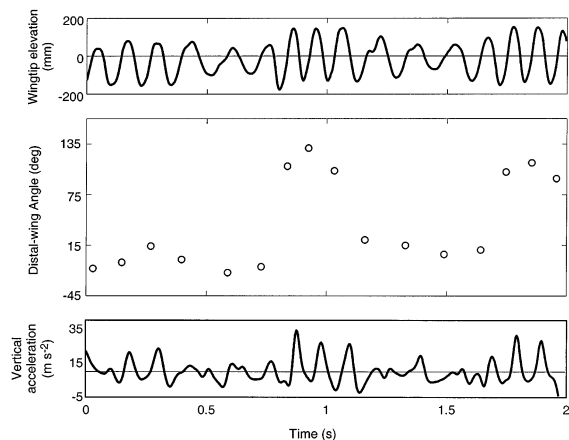


Fig. 2. Wing and body kinematics, including vertical-axis wing-tip motion, distal-wing angle, and vertical acceleration of the body, during two seconds of flight in a ringed turtle-dove flying at an average equivalent airspeed of 7 m s⁻¹. Variation in acceleration of the body was associated with changes in wingbeat amplitude, frequency, and distal-wing angle relative to the mid-line of the body. This type of non-steady flight behavior was typical of all four bird species used in the study during flight at intermediate speeds.

altered wingbeat amplitude, frequency, and wing-span at mid-upstroke in association with changes in flight velocity and altitude as previously reported by Tobalske and Dial (1996) and Tobalske et al. (1997).

Slow flight in all of the species was associated with several kinematic patterns. These included: (i) increased body angle, (ii) increased tail spreading at mid-downstroke, (iii) decreased stroke-plane angle relative to horizontal, (iv) increased total wing excursion (Fig. 1C and Fig. 3). In the species that used tip-reversal during upstroke, the wingtip path gives rise to a “figure-8” pattern in lateral projection (Dathe and Oehme 1978, Scholey 1983, Tobalske and Dial 1996, 2000; Fig. 3). Changes in these parameters occurred gradually across speeds, similar to the patterns reported in Tobalske and Dial (1996). Compared with slow flight, when flying at equivalent airspeeds $\geq 11 \text{ m s}^{-1}$ (Fig. 3B), all of the

species reduced their tail spread and used lower-amplitude wingbeats, in which the tip moved in an elliptical arc with a stroke-plane angle approaching a vertical orientation relative to the bird's body.

Wing-tip and wrist spans at mid-downstroke varied only slightly among flight speeds for each of the species, and consistent patterns over a range of speeds were not evident (Fig. 4). In contrast, mid-upstroke tip span tended to decrease in all four species and mid-upstroke wrist span tended to increase as flight speed increased. During upstroke, the magpies tended to adduct their entire wings proportionately more than the other species at all speeds. This was evident in the relatively small tip and wrist spans that magpies adopted at mid-upstroke over the full range of speeds (Fig. 4). Hence, the fundamental difference observed between magpies that use a highly-flexed, “feathered” upstroke and the three other species, all of which use wing-tip reversal upstrokes at equivalent speeds ≤ 7 to 9 m s^{-1} , is that wing-tip spans were relatively great at mid-upstroke during slow flight in the three species using tip-reversal.

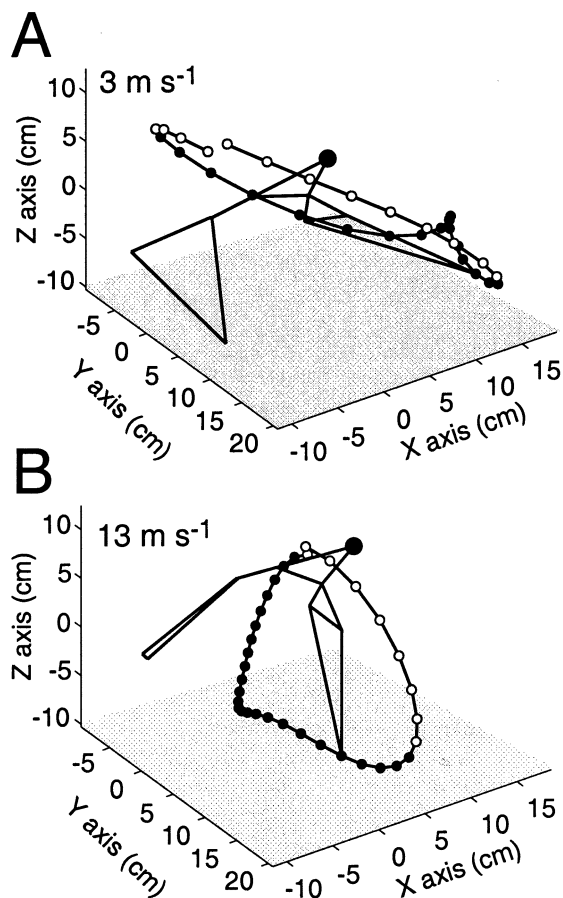


Fig. 3. Three-dimensional graphs of wingtip paths during a representative wingbeat in a ringed turtle dove flying at A) 3 m s^{-1} and B) 13 m s^{-1} in the wind tunnel. Stick figures represent the instantaneous location of anatomical markers on the bird, and reveal body, wing, and tail posture at mid-upstroke. The “figure-8” wingtip path at slow speeds, indicating a wingtip-reversal upstroke, was also observed in budgerigars and cockatiels, but not magpies.

Discussion

Our analysis provides new comparative data which suggest that the transition speed from a wing-tip reversal upstroke to a swept-wing upstroke occurs near an equivalent airspeed of 9 m s^{-1} in cockatiels and doves, and $9\text{--}11 \text{ m s}^{-1}$ in the budgerigar (Fig. 1). These results are reasonably consistent with a transition speed of 10 m s^{-1} reported for the 330 g pigeon (Tobalske and Dial 1996). Thus, our results indicate that birds, differing in body mass by an order of magnitude ($10\times$), transition between a tip-reversal and swept-wing upstroke at approximately the same (equivalent) airspeed (Fig. 1).

If tip-reversal contributes an aerodynamic function, helping to support body weight by generating useful lift during the upstroke, it may be that the higher distal wing angles in the doves relative to budgerigars and cockatiels are due to relatively higher disc loading in the doves. Higher disc loading should signal higher induced power requirements and a proportionally greater need for attention to weight support during slow flight (Rayner 1979, Norberg 1990). The distinct behavior of the magpie, which uses feathered upstroke at all steady flight speeds, appears to be related to its comparatively broad wings (Table 1). Magpies are within the range of wing and disc loading exhibited by the other three species in this study, but their average wing chord is higher and their aspect ratio is lower.

Although the magpie is the largest species in our present study, its use of feathered upstrokes is not explained by its body mass. Zebra finch *Taeniopygia*

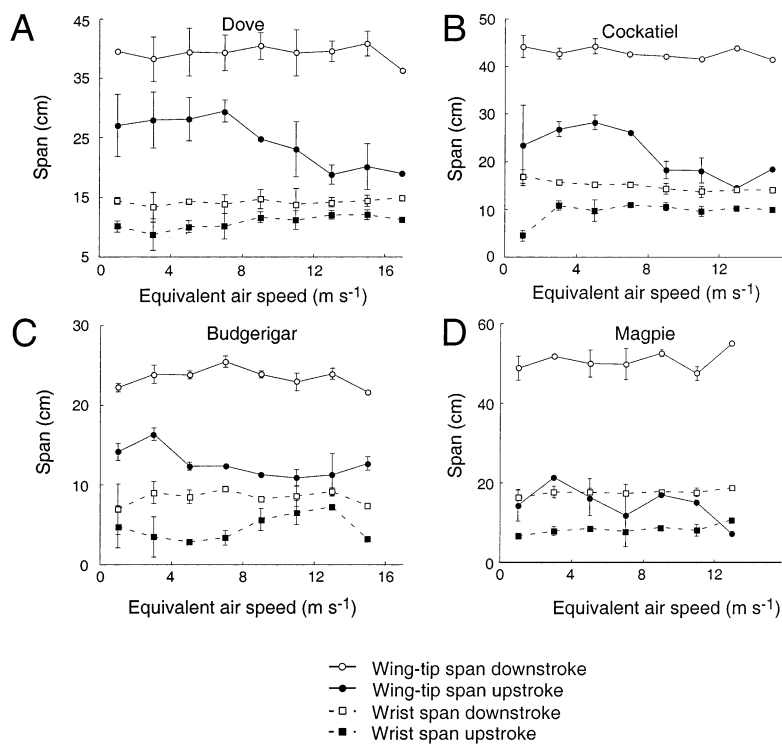


Fig. 4. Wing-tip and wrist spans at mid-downstroke and mid-upstroke, as a function of flight speed, in four species flying in the wind tunnel: budgerigars, cockatiels, ringed turtle doves, and black-billed magpies. Error bars represent ± 1 S.D.

guttata are smaller than all the species in the present study, (13 g; Tobalske et al. 1999), yet they use a feathered upstroke across a broad range of speeds (0–14 m s⁻¹). Aspect ratio in the zebra finch is 4.5, which strongly suggests that a low aspect ratio is related to the use of feathered upstrokes.

The aerodynamic significance of different upstroke patterns is not well understood, in part because synchronized kinematic and aerodynamic measurements are not yet available. Results from vortex-visualization studies of flight in finch *Fringilla* spp. (Kokshaysky 1979), pigeon (Spedding et al. 1984), and jackdaw *Corvus monedula* (Spedding 1986) indicate that upstrokes are aerodynamically inactive in slow flight. Wing motion was not documented in these studies, but kinematics of slow flight in the same or in related species (e.g. Brown 1953, Dathe and Oehme 1978, Tobalske and Dial 1996, Tobalske et al. 1999), suggest that these species use either feathered or tip-reversal upstrokes during slow flight. The pulsatile nature of lift production at lower flight speeds has been argued to give rise to a vortex-ring structure in the wake (Rayner 1991, 1995). In contrast, other empirical data, obtained using kinematics, strain gauges, and/or accelerometers, suggest that the wing may produce useful lift or drag during tip-reversal upstroke (Corning and Biewener 1998, Warrick and Dial 1998, Seveyka 1999). Even if most of upstroke is inactive with regard to lift or drag, one function of tip-reversal during upstroke may be to increase lift production during the subsequent down-

stroke by producing bound circulation on the wing *via* wing rotation prior to the start of the kinematically-defined downstroke (Rayner 1995, Tobalske 2000). This would offset the timing of the 'Wagner effect' (Vogel 1994) in which lift production does not reach a maximum until an airfoil has traveled for several chord lengths away from a starting vortex. It is expected that lift is generated during swept-wing upstrokes, but this interpretation is based largely on one study of the European kestrel *Falco tinnunculus* in free flight (Spedding 1987) that did not examine wing kinematics.

All four species that we studied showed considerable variation in altitude and velocity during flight at intermediate speeds. This variation appeared to be related to variation in wing and body kinematics, including tip-reversal angle (Fig. 2). Similar variation was previously reported for pigeons and magpies flying in a wind tunnel (Tobalske and Dial 1996). This may represent normal flight behavior or, alternatively, an artifact associated with flight in a closed-jet wind tunnel. At least for the magpie, similar variation in altitude and velocity is apparent when comparing flight in a wind tunnel with free flight outdoors (Tobalske et al. 1997). A challenge for future research will be to test whether birds that use a tip-reversal upstroke during slow flight regularly vacillate between accelerative and decelerative wingbeats during flight at equivalent speeds of 7–9 m s⁻¹ outdoors.

Tunnel effects are predicted to vary according to the ratio of wingspan to working section diameter (Rayner

1994, Barlow et al. 1999). Wall effects in a closed-jet wind tunnel should decrease characteristic speeds such as minimum power or maximum range speed (Rayner 1994), but their potential effects on wing kinematics have not been studied. The largest of the species used in the present study, the black-billed magpie (Table 1), had a wingspan that was only 50% of the flight chamber diameter. Our data are consistent with a previous study (Tobalske and Dial 1996) of magpie flight kinematics in a tunnel that has a working section 75 cm in diameter compared with 120 cm for the tunnel used in our current study. Thus, magpies exhibit similar basic patterns of flight behavior and wing kinematics regardless of substantial differences in tunnel size.

Transitions from tip-reversal to swept-wing upstrokes has received relatively little study in the context of free flight conditions. Brown (1953) documented the transition from a wing-tip reversal upstroke to a feathered, "transitional" upstroke that occurs with increasing flight speed in pigeons. Brown demonstrated that a feathered upstroke, without tip reversal, is used at 12.4 m s⁻¹ in free flight. However, it is not clear from his analysis whether such an upstroke may be used at slower speeds. Transitional wingbeats occur at 10 m s⁻¹ in pigeons flying in a wind tunnel (Tobalske and Dial 1996) and at 9 or 11 m s⁻¹ in budgerigars, cockatiels, and doves in the present study (Fig. 1). These data hint that transitions between wingbeat styles may occur at slower speeds in a wind tunnel compared with free flight, possibly due to more restricted space or wall effects.

Consequently, additional comparative study of flight kinematics, focusing upon transitions between wingbeat styles in the field, is warranted. Fortunately, an important value of our basic kinematic measurements of tip-reversal angle (Fig. 1), and wing- and wrist-spans at mid-upstroke, is that these may be obtained from single-camera views of birds in flight outdoors (Scholey 1983, Tobalske 1996, Tobalske et al. 1997; Figs. 1 and 4). As we have shown here and in previous studies (Tobalske and Dial 1996, 2000, Tobalske 2000), a combination of distal-wing angle and wingspan at mid-upstroke facilitates identification of wingbeat styles in birds when studying their flight behavior in the field. Specifically, tip-reversal upstrokes are characterized by a mid-upstroke distal-wing angle that exceeds 20°, together with relatively great wing-tip spans and small wrist spans. Faster flight in those species that use a tip-reversal during slow flight is characterized by a distal-wing angle near 0°, small wing spans at mid-upstroke, and wrist spans at mid-upstroke that approach the mid-downstroke wrist span (Tobalske and Dial 1996; Fig. 4). In contrast, the magpie appears representative of species that use a feathered upstroke, with a highly flexed-wing during flight over its observed full range of steady speeds. Upstrokes characteristic of this style of wingbeat feature a distal-wing angle < 20°, and

wrist and tip spans that are relatively small compared with the same spans during downstroke.

Acknowledgements – We wish to thank Matt Bundle and Ken Dial for the loan of well-trained magpies. Support for the kinematic analysis of bird flight was provided by grants from the NSF (IBN-0090265) and the Murdock Charitable Trust (99153).

References

- Barlow, J. B., Rae, W. H., Jr. and Pope, A. 1999. *Low-speed Wind Tunnel Testing*, 3rd ed. – Wiley-Interscience, New York.
- Brown, R. H. J. 1953. The flight of birds. II. Wing function in relation to flight speed. – *J. Exp. Biol.* 30: 90–103.
- Brown, R. H. J. 1963. The flight of birds. – *Biol. Rev.* 38: 460–489.
- Corning, W. R. and Biewener, A. A. 1998. *In vivo* strains in pigeon flight feather shafts: implications for structural design. – *J. Exp. Biol.* 201: 3057–3065.
- Dathe, H. H. and Oehme, H. 1978. Typen des Ruttelfluges der Vögel. – *Biol. Zbl.* 97: 299–305.
- Hatze, H. 1988. High-precision three-dimensional photogrammetric calibration and object space reconstruction using a modified DLT-approach. – *J. Biomechanics* 21: 533–538.
- Hedrick, T. L., Tobalske, B. W. and Biewener, A. A. 2002. Estimates of circulation and gait change based on a three-dimensional kinematic analysis of flight in cockatiels (*Nymphicus hollandicus*) and ringed turtle-doves (*Streptopelia risoria*). – *J. Exp. Biol.* 205: 1389–1409.
- Hoerner, S. 1935. Tests of Spheres With Reference to Reynolds Number, Turbulence, and Surface Roughness. Technical Memorandum No. 777. – National Advisory Committee for Aeronautics, Langley, Virginia.
- Kokshaysky, N. V. 1979. Tracing the wake of a flying bird. – *Nature* 279: 146–148.
- Norberg, U. M. 1990. *Vertebrate Flight: Mechanics, Physiology, Morphology, Ecology and Evolution*. – Springer-Verlag, Berlin.
- Park, K. J., Rosén, M. and Hedenström, A. 2001. Flight kinematics of the barn swallow (*Hirundo rustica*) over a wide range of speeds in a wind tunnel. – *J. Exp. Biol.* 204: 2741–2750.
- Pennycuik, C. J. 1989. *Bird Flight Performance: A Practical Calculation Manual*. – Oxford University Press, New York.
- Pennycuik, C. J., Alerstam, T. and Hedenström, A. 1997. A new low-turbulence wind tunnel for bird flight experiments at Lund University, Sweden. – *J. Exp. Biol.* 200: 1441–1449.
- Rayner, J. M. V. 1979. A new approach to animal flight mechanics. – *J. Exp. Biol.* 80: 17–54.
- Rayner, J. M. V. 1991. Wake structure and force generation in avian flapping flight. – *Acta XX Congr. Internat. Ornithol.*, Volume II., pp. 702–715.
- Rayner, J. M. V. 1994. Aerodynamic corrections for the flight of birds and bats in wind tunnels. – *J. Zool. Lond.* 234: 537–563.
- Rayner, J. M. V. 1995. Dynamics of the vortex wakes of flying and swimming vertebrates. – In: Ellington, C. P. and Pedley, T. J. (eds). *Biological Fluid Dynamics*. Symposia of the Society for Experimental Biology XLIX. The Company of Biologists Limited, Cambridge, pp. 131–155.
- Scholey, K. D. 1983. *Developments in vertebrate flight: climbing and gliding of mammals and reptiles and the flapping flight of birds*. – PhD thesis, University of Bristol.
- Seveyka, J. J. 1999. *Effects of body size and morphology on the flight behavior and escape flight performance of birds*. – MS thesis, University of Montana.

- Spedding, G. R. 1986. The wake of a jackdaw (*Corvus monedula*) in slow flight. – J. Exp. Biol. 125: 287–307.
- Spedding, G. R. 1987. The wake of a kestrel (*Falco tinnunculus*) in flapping flight. – J. Exp. Biol. 127: 59–78.
- Spedding, G. R., Rayner, J. M. V. and Pennycuik, C. J. 1984. Momentum and energy in the wake of a pigeon (*Columba livia*) in slow flight. – J. Exp. Biol. 111: 81–102.
- Tobalske, B. W. 1996. Scaling of muscle composition, wing morphology, and intermittent flight behavior in woodpeckers. – Auk 113: 151–177.
- Tobalske, B. W. 2000. Biomechanics and physiology of gait selection in flying birds. – Physiol. Biochem. Zool. 73: 736–750.
- Tobalske, B. W. and Dial, K. P. 1996. Flight kinematics of black-billed magpies and pigeons over a wide range of speeds. – J. Exp. Biol. 199: 263–280.
- Tobalske, B. W. and Dial, K. P. 2000. Effects of body size on take-off flight performance in the Phasianidae (Aves). – J. Exp. Biol. 203: 3319–3332.
- Tobalske, B. W., Olson, N. E. and Dial, K. P. 1997. Flight style of the black-billed magpie: variation in wing kinematics, neuromuscular control, and muscle composition. – J. Exp. Zool. 279: 313–329.
- Tobalske, B. W., Peacock, W. L. and Dial, K. P. 1999. Kinematics of flap-bounding flight in the zebra finch over a wide range of speeds. – J. Exp. Biol. 202: 1725–1739.
- Vogel, S. 1994. Life in moving fluids: the physical biology of flow, 2nd ed. – Princeton Univ. Press, Princeton, New Jersey.
- Walker, J. A. 1998. Estimating velocities and accelerations of animal locomotion: a simulation experiment comparing numerical differentiation algorithms. – J. Exp. Biol. 201: 981–985.
- Warrick, D. R. and Dial, K. P. 1998. Kinematic, aerodynamic and anatomical mechanisms in the slow, maneuvering flight of pigeons. – J. Exp. Biol. 201: 655–672.
- Woltring, H. J. 1986. A Fortran package for generalized cross-validatory spline smoothing and differentiation. – Adv. Eng. Soft. 8: 104–113.

(Received 11 February 2002, revised 19 September 2002, accepted 22 September 2002.)